A Novel TBX1 Variant Causing Hypoparathyroidism and Deafness

Malak Alghamdi,[1] Reem Al Khalifah,[2] Doua K. Al Homyani,[3] Waleed H. Alkhamis,[4] Stefan T. Arold,[5] Aishah Ekhzaimy,[6] Mohammed El-Wetidy,[7] Tarek Kashour,[8] and Rabih Halwani[9,10]

[1]*Medical Genetic Division, Department of Pediatrics, College of Medicine, King Saud University, Riyadh 4545, Saudi Arabia;* [2]*Pediatric Endocrinology Division, Department of Pediatrics, College of Medicine, King Saud University, Riyadh 4545, Saudi Arabia;* [3]*Pediatric Endocrinology, Department of Pediatrics, College of Medicine, King Saud University, Riyadh 4545, Saudi Arabia;* [4]*Department of Obstetrics and Gynecology, King Saud University Medical City, Riyadh 4545, Saudi Arabia;* [5]*Computational Bioscience Research Center (CBRC), Division of Biological and Environmental Sciences and Engineering (BESE), King Abdullah University of Science and Technology (KAUST), Thuwal, 23955–6900, Saudi Arabia;* [6]*Adult Endocrinology, Department of Medicine, College of Medicine, King Saud University, Riyadh 4545, Saudi Arabia;* [7]*College of Medicine Research Center, King Saud University, Riyadh 4545, Saudi Arabia;* [8]*Cardiology Department, College of Medicine, King Saud University, Riyadh 4545, Saudi Arabia;* [9]*Sharjah Institute for Medical Research (SIMR), Department of Clinical Sciences, College of Medicine, University of Sharjah, P.O. Box 27272, Sharjah, United Arab Emirates; and* [10]*Immunology Research Laboratory, Department of Pediatrics, College of Medicine, King Saud University, Riyadh 4545, Saudi Arabia.*

ORCiD numbers: 0000-0002-8317-5951 (M. Alghamdi); 0000-0002-5304-3528 (R. Al Khalifah); 0000-0003-1774-2388 (W. H. Alkhamis); 0000-0001-5278-0668 (S. T. Arold).

Background. The TBX1 gene encodes the T-box 1 protein that is a transcription factor involved in development. Haploinsufficiency of the TBX1 gene is reported to cause features similar to DiGeorge syndrome. The TBX1 gene is located within the DiGeorge syndrome region, and studies support that the TBX1gene is responsible for most of the features of the phenotype of hemizygous deletion of chromosome 22q11.2. In this study, we report a family of 4 (a father with 3 children) who presented with congenital hypoparathyroidism and hypocalcemia, facial asymmetry, deafness, normal intelligence, and no cardiac involvement.

Methods. We performed whole genome sequencing, computational structural analysis of the mutants, and gene expression studies for all affected family members.

Results. Whole genome sequencing revealed a paternal inherited novel heterozygous variant, c.1158_1159delinsT p.(Gly387Alafs*73), in the exon 9 isoform C TBX1 gene, causing a loss of nuclear localization sequence (NLS) and transactivation domain (TAD) with no change in gene expression and resulted in a DiGeorge-like phenotype.

Conclusion. A pathogenic variant in the TBX1 gene exon 9 C that predicted to cause a loss in the NLS region and most of TAD leads to variable features of hypoparathyroidism, distinctive facial features, deafness, and no cardiac involvement. In addition, our report and previous reports indicate the presence of a wide phenotypic spectrum of TBX1 genetic variants and the consistent absence of cardiac involvement in the case of pathogenic variants on exon 9 isoform C TBX1 gene.

22q11.2 deletion syndrome is considered one of the most common microdeletional syndromes in humans, which presents with a wide spectrum of phenotypes ranging from mild adulthood onset to severe neonatal presentations (1, 2). The prevalence is up to 14/100 000 births, with a mean age of diagnosis at 5 years (3). DiGeorge syndrome is a contiguous gene syndrome caused by a 1.5–3 Mb microdeletion of 22q11.2 (4). DiGeorge syndrome (conotruncal anomaly face syndrome or velocardiofacial syndrome) presents with variable phenotypes, including variable cardiovascular manifestations, endocrine manifestations with hypoparathyroidism, hypothyroidism and thymic hypoplasia, cleft palate and nasal speech, and central nervous system (CNS) features with delayed psychomotor development associated with characteristic facial features (1, 2) One of the 30–40 genes deleted in this condition is the TBX1 gene, and there is accumulating evidence that this gene is responsible for most of the phenotype of the 22q11.2 deletion (5–7). Moreover, several studies described the TBX1 variants as a causative genetic defect for DiGeorge syndrome because these TBX1 variants cause a similar phenotype without microdeletion (6–11).

DiGeorge syndrome caused by a pathogenic variant in the TBX1 gene is a rare autosomal dominant disease that is associated with variable degrees of pathological phenotypes. The TBX1 protein encoded by the TBX1 gene is a member of the conserved T-box transcription factor family and can act as a gene enhancer or repressor in transcriptional regulation of developmental processes (12). It has been demonstrated that TBX1 mutations resulted in 1 of 5 phenotypes of 22q11.2, namely, deletion including conotruncal anomaly face syndrome, cardiac defect, velopharyngeal insufficiency, thymic hypoplasia, or hypoparathyroidism. Intellectual disability and psychomotor retardation are not consistent features of TBX1 mutations (6–11). Several TBX1 variants have been described as disease-causing variants through both loss and gain-of-function mutations (10). (Table 1).

Further studies revealed that TBX1 has three isoforms that share exons 1–8 but differ in exons 9, 9A, 9B/10, and 9C. Of these 3 isoforms, TBX1C is the main transcript in mice, and it has been shown in humans that the mutation in TBX1C results in features similar to the 22q11.2 deletion (13–15).

Here, we report a family of 4 presenting with hearing loss, hypoparathyroidism, facial asymmetry, nasal speech, and dysmorphic features, with no other congenital cardiac anomaly and with normal intellectual function. Whole genome sequencing uncovered a novel TBX1 variant, c.1158_1159delinsT p.(Gly387Alafs*73), which is consistent with a genetic diagnosis of a TBX1-associated phenotype with an autosomal dominant mode of inheritance.

A. Case III-C

A 5-year-old boy was diagnosed with hypoparathyroidism at the age of 1 month when he had neonatal seizures. He is also known for speech delay and bilateral sensory neural hearing loss (SNHL). He was followed-up at a peripheral hospital and was on 1 alpha calcidiol drop only. He presented to our emergency room (ER) with a history of vomiting, abdominal pain, and numbness of hands for 1 day after he visited our cochlear transplantation center.

He was born at 40 weeks of gestation via normal spontaneous vaginal delivery to a 31-year-old healthy mother and 33-year-old father (see Fig. 1). The antenatal course was normal, followed by an unremarkable perinatal course with a birth weight of 2700 g. His father and two of his siblings had the same presentation (cases II-C, III-A, III-B). The physical examination showed a weight of 17.6 kg (25th percentile), a height of 109.6 cm (50th percentile), and a head circumference of 51 cm (25th–50th percentile). He has mild facial dysmorphism in the form of a prominent nose with a bulbous tip, small mouth and eyes, ocular hypertelorism, low-set ears, and a long face (see Fig. 1A). The chest, cardiac, and abdominal examination findings were unremarkable. He had a positive Chvostek sign. Investigations upon presentation to the ER showed total serum calcium concentration of 1.28 mmol/L (normal range 2.20–2.70), corrected calcium of 1.32 mmol/L, serum phosphate of 2.31 mmol/L (normal 1.12–1.45 mmol/L), magnesium (Mg) of 0.63 mmol/L, and alkaline

Table 1.   Reported TBX1 Gene-Related Phenotypes

References		Cono-truncal anomaly	Endocrine	Immunology	Craniofacial	Velopharyngeal	Deafness	Psycho-developmental	Others	Variant	Predicted effect
										Molecular Genetic	
Yagi et al (2003)	F-1	TOF/PA	-ve	-ve	+ve	+ve	-ve	Normal		F148Y	GoF
	F-2	IAA/VSD	+ve	+ve	+ve	+ve	+ve	Normal		G310S	GoF
	F-3- I	TOF/RAA	-ve	+ve	+ve	-ve	-ve	Normal		1223delC	LoF
	II	-ve	-ve	-ve	+ve	+ve	-ve				
	III	-ve	+ve	-ve	+ve	+ve	-ve				
Paylor et al (2006)	F-4-I	Negative	NA	NA	Characteristic facial appearance of VCFS and hyper-nasal speech	NA	NA	Depression / normal IQ		23-bp frameshift deletion (1320-1342del23bp)	LoF
	II	TOF						Asperger syndrome / normal IQ			
	III	Pulmonary stenosis						Social anxiety/ normal IQ			
Zweier et al (2007)	F-5-I	-ve	-ve	-ve	+ve	-ve	-ve	DD	Short stature	H194Q	GoF
	-II	-ve	-ve	-ve	+ve	-ve	-ve	Normal	Short stature		
Rauch et al (2010)	F-6-I	TOF/VSD/ absent Pulmonary veins			Facial asymmetry			Normal	Scoliosis Frequent infections	c.1399-1428dup30	LoF
Ogata et al (2014)	F-7-I	-ve	+ve	-ve	+ve	+ve	+ve	DD	Graves disease	c.1253delA, p.Y418fsX459	Loss of NLS
	II	-ve	-ve	NA	+ve	+ve	-ve	DD			
	III	-ve	+ve	NA	+ve	+ve	-ve	DD			
	IV	-ve	-ve	NA	+ve	+ve	-ve	DD			
	V	-ve	+ve	NA	+ve	+ve	-ve	DD			
Hasegawa et al (2018)	F-8	-ve	+ve	Thymic hypoplasia	-ve	-ve	-ve	Normal	Postaxial polydactyly of the right fifth toe	c.967_977dup AACCCCGTGGC	LoF
Our family	III-C	-ve	+ve	-ve	+ve	-ve	+ve	Normal		c. 1158_1159delinsT p.(Gly387Alafs*73)	Loss of NLS
	III-B	-ve	+ve	-ve	+ve	-ve	+ve	DD		c.1158_1159delinsT p.(Gly387Alafs*73)	Loss of NLS
	III-A	-ve	+ve	-ve	+ve	-ve	+ve	Normal		c.1158_1159delinsT p.(Gly387Alafs*73)	Loss of NLS
	II-C	-ve	+ve	-ve	+ve	-ve	-ve	Normal		c.1158_1159delinsT p.(Gly387Alafs*73)	Loss of NLS

Abbreviations: DD, developmental delay; GoF, gain of function; LoF, loss of function.
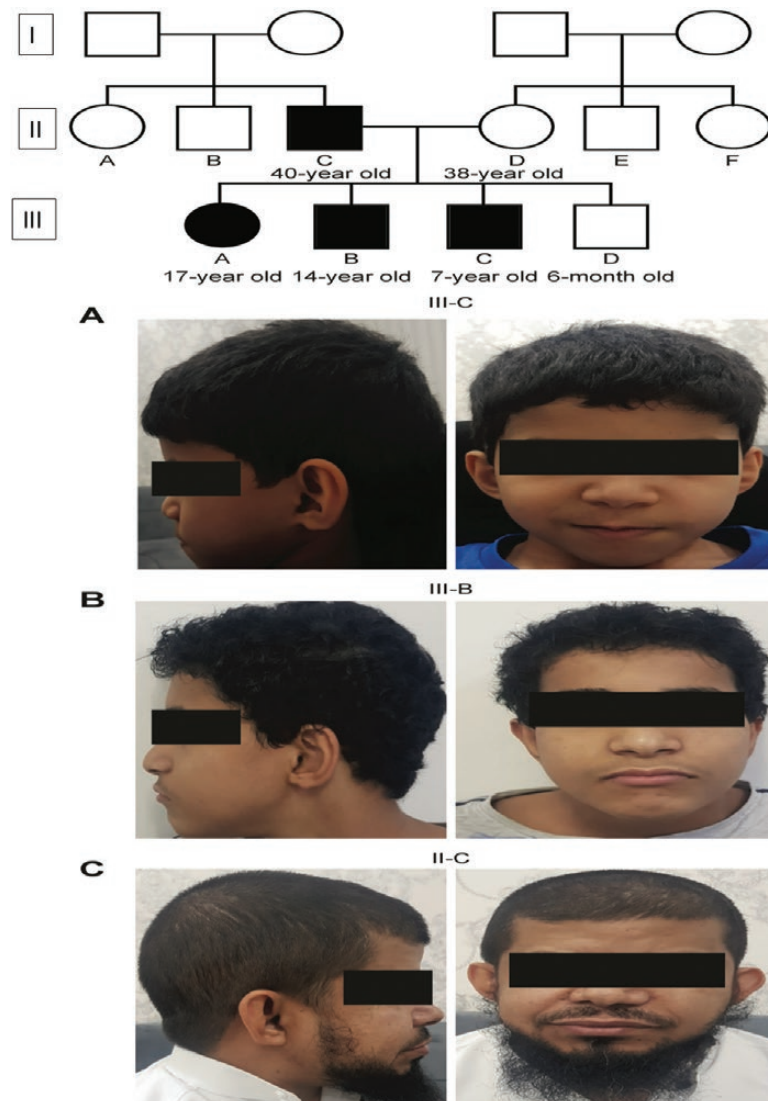
Figure 1. Family pedigree and the distinctive facial features of the affected individuals.

phosphatase (ALP) of 185 unit/l. The serum parathyroid hormone (PTH) concentration was low at 3.8 pg/ml (normal range15–65 pg/ml), 25-hydroxyvitamin D (25[OH]D) was 119 nmol/l (normal 75–125 nmol/l), and he had a normal urinary calcium:creatinine ratio. The following parameters were normal: blood absolute T lymphocyte subsets, serum thyroid stimulating hormone, and serum free thyroxin. The patient was admitted to the pediatric intensive care unit (PICU) due to a prolonged QT interval (in ECG) secondary to hypocalcemia and was managed with intravenous calcium gluconate.

An ultrasound of the abdomen showed normal kidney size, shape, echogenicity, and parenchymal thickness, with no hydronephrosis or renal stones. An electrocardiogram performed during hypocalcemia showed a prolonged QT interval with a normal Holter monitor. Cardiac echography showed normal cardiac anatomy, and he had a normal skeletal survey. A computed tomography (CT) scan of the temporal bone showed congenital deformity of the cochlea and vestibules with cystic communication between the middle and apical cochlear turns and dilated vestibules with hypoplastic semicircular canal. Magnetic resonance imaging (MRI) revealed bilateral underdevelopment of inner ear structures, with normal cochlear nerve bilaterally. After controlling his calcium level, the patient underwent

cochlear implants. Whole genome sequencing (WGS) revealed a heterozygous likely pathogenic variant identified in the TBX1 gene, variant c.1158_1159delinsT p.(Gly387Alafs*73).

Currently, at the age of 7 years, he is on elemental calcium (57 mg/kg/day) and l-alphacalcidiol (one mcg daily). His latest investigations and his growth parameters were normal.

B. Case III-B

A 12-year-old boy was diagnosed with hypoparathyroidism incidentally. During the admission of his youngest brother (Case III-C) with acute hypocalcemia, we evaluated him for hypoparathyroidism because he had bilateral SNHL and similar dysmorphic features. Upon evaluation, the mother gave a history of two seizures in the context of fever that did not require treatment and one incidental hypocalcemia at the age of 2 years found during routine blood investigations, for which he was given calcium supplementation for less than 1 month and then it was stopped. Since stopping the calcium supplements, he reports negative symptoms and signs for hypocalcemia. During admission, he was found to have a prolonged QT interval and severe hypocalcemia that was managed with an intravenous calcium gluconate infusion.

He was born at 38 weeks by spontaneous vaginal delivery, with a birth weight of 2.7 kg. The developmental milestones were reported to be delayed, and he is currently attending a special needs school. A physical examination showed hypertelorism, downward slanting palpebral fissures, bulbous nose, and low-set ears (See Fig. 1B). His height was 161.4 cm (31.44 percentile), weight was 57 kg (67.66 percentile), and body mass index (BMI) was 21.88 kg/m2 (79.32 percentile). He had a positive Chvostek sign. Other systemic examinations were normal. Laboratory investigations revealed total serum calcium concentration of 1.48 mmol/L, corrected calcium of 1.58 mmol/L, phosphate of 3.32 mmol/L, magnesium of 0.76 mmol/L, 25(OH)D of 65.1 nmo/l, and PTH of 0.53 pg/ml. Blood absolute T lymphocyte subsets, serum thyroid stimulating hormone (TSH), serum free thyroxin (FT4) were normal. Brain MRI showed severe malformation of the cochlea. Currently, at the age of 14 years, he is on 42 mg/kg/day of elemental calcium and on 1.25 mcg of calcitriol twice daily. His current total serum calcium concentration is 2.09 mmol/L, corrected calcium is 2.13, phosphate is 2.56 mmol/L, magnesium is 0.7 mmol/L, and 25(OH)D is 71.63 nmo/l.

C. Case III-A

A 14-year, 6-month-old sister of cases III-B and III-C was evaluated for bilateral SNHL and hypocalcaemia following the hospitalization of case III-C. Unfortunately, at the age of 1 year, she was treated for recurrent otitis media as a presumed cause of hearing impairment until the age of 3 years. She had history of seizures at age of 3 years and at age of 12 years; at that time hypoparathyroidism was not diagnosed. Evaluation of inner ear pathology by MRI revealed bilateral congenital deformity of the inner ear structures, an absent left cochlear nerve, and the right is significantly small. Temporal bone computed tomography revealed slightly hypoplastic internal auditory canals. During the preoperative assessment of the cochlear implant, she was found to have prolonged QT interval secondary to hypocalcemia. Holter monitoring was performed for 24 hours and was normal. then she was referred to an adult endocrinology for follow-up.

She was born at term via spontaneous vaginal delivery, with normal antenatal and perinatal courses. Her birth weight was 3 kg. A physical examination showed low-set ears, delayed eruption of adult teeth, and normal development. Weight was 51.1 kg (5th percentile), height was 146.2 cm (< 3rd percentile), and head circumference was 54.5 cm (50th percentile). She had negative Chvostek sign and Trousseau signs. The chest, cardiac, and abdominal examination findings were all unremarkable. The serum total calcium concentration was low at 1.82 mmol/L, corrected calcium was at 1.86 mmol/L, serum phosphate was at 1.96 mmol/L, 25(OH)D was at 62.52 nmol/L, and PTH was at 0.679 pg/ml. She had a normal thyroid function test. A renal ultrasound showed that both kidneys were normal

in size, shape, and position, and were normal cortical thickness and echogenicity, with no evidence of stones, hydronephrosis, or renal masses. Audiology screening showed severe profound bilateral sensory neural hearing loss. A skeletal survey showed no deformities. Currently, at the age of 16 years, she is on l-alpha-calcidiol, 1 mcg twice a day and 600 mg calcium carbonate twice a day. Her last evaluation revealed a total corrected calcium of 2.21 mmol/L, phosphorus of 1.9 mmol/L, and her growth parameters were as follows: weight was 44.6 kg (< 25th percentile) and her height was 152 cm (5th percentile).

D. Case II-C

The father is 39 years old and was diagnosed with hypoparathyroidism at 4 years old. He presented to a peripheral hospital with a low calcium level leading to seizure. Since then, he had been having recurrent symptoms of perioral numbness, blacking out, and seizures. His symptoms were relieved with an intermittent calcium infusion during emergency department visits. He had no regular follow-up for his hypocalcemia and he had not been on regular calcium or vitamin D replacement since the age of 4 years. He had been complaining of delayed eruption of adult teeth. He is not known to have SNHL, but he has conductive hearing impairment.

He is married to a non-consanguineous healthy female (see Fig. 1) His parents, siblings, and second-degree relatives did not have a history of SNHL, hypocalcemia, sudden death, or cardiac diseases. He was referred to an adult endocrinology clinic during the hospitalization for Case III-C. At the first visit in our adult endocrinology clinic, his calcium level was 1.98 mmol/L, corrected calcium was 2.00 mmol/L, phosphorus level was 1.62 mmol/L, and 25(OH)D was 32.2 nmol/L. He has a normal thyroid function test and immunological studies. He was seen at the otolaryngology clinic because he was complaining of left ear pain and nasal obstruction for a long time, and he was diagnosed with a left ear central perforation and nasal deformity. He had a normal hearing assessment, with no mental or developmental delay.

On physical examination, he has low-set prominent ears, facial asymmetry, absent adult teeth, nasal speech, and a bulbous nose (See Fig. 1C). His height was 156 cm (< 3rd percentile), and his weight was 72 kg with a BMI of 29.24. He was started on 1200 mg of regular calcium carbonate three times daily, 1 mcg of 1-alpha twice daily, and 1 mcg l-alpha-calcidiol daily. Since then, he has normal calcium levels and no further symptoms of hypocalcemia. During his last visit, his total calcium level was 2.34 mmol/L, and his corrected calcium level was 2.36 mmol/L and his phosphorus level was 1.69 mmol/L.

1. Materials and Methods

A. Whole Genome Sequencing

Genomic DNA was fragmented by sonication, and Illumina adaptors were ligated to generated fragments for subsequent sequencing on the HiSeqX platform (Illumina) to yield an average coverage depth of ~30X. An end-to-end in-house bioinformatics pipeline, including base calling, primary filtering of low quality reads, and probable artifacts, and annotation of variants was applied. Copy number variant (CNV) calling is based on the HAS pipeline. All disease-causing variants reported in HGMD® and ClinVar or in CentoMD®, in addition to all variants with minor allele frequency (MAF) of less than 1% in the gnomAD database were considered. Evaluation is focused on coding exons, along with flanking +/-20 intronic bases—however, extended to the complete gene region for candidate genes or in search for a second previously described variant in AR inheritance pattern. All pertinent inheritance patterns are considered. In addition, provided family history and clinical information are used to eventually evaluate identified variants. All identified variants were evaluated with respect to their pathogenicity and causality. All variants related to the phenotype of the patient, except benign or likely benign variants, are reported. CNVs of unknown significance

are not reported. Reported CNVs are confirmed with another method, such as MLPA and quantitative polymerase chain reaction (qPCR). Variants of relevance identified by next generation sequencing (NGS) are continuously and individually validated in-house for quality aspects; those variants that meet our internal quality control (QC) criteria (based on extensive validation processes) are not validated by Sanger. To study mutations indicated by exome sequencing, Sanger sequencing was performed for all family members.

B. Computational Structural Analysis of Mutants

MUSCLE (www.ebi.ac.uk/Tools/msa/muscle) was used for sequence alignments. RaptorX was used to produce homology models and to predict secondary structures and disorders (16). The eukaryotic linear motif (ELM) resource was used for the identification of functional sites in proteins (17).

C. Gene Expression Studies

Ribonucleic acid was extracted from the peripheral blood mononuclear cell (PBMC) of all family members. The isolated RNA was reverse-transcribed into cDNA using the M-MLV reverse transcriptase assay (Promega Corporation, Maddison, WI). Real-time polymerase chain reaction (PCR) amplification of the obtained cDNA targets was performed using the Power SYBR Green PCR Kit (Applied Biosystems). Specific cDNA primers (Integrated DNA Technologies, Leuven, Belgium) were used to determine the expression of TBX1. The expression was determined using the 7900HT fast real-time quantitative PCR system (Applied Biosystems, CA, USA). The relative expression of all genes of interest were normalized to glyceraldehyde 3-phosphate dehydrogenase (GAPDH) and determined by the ΔΔCt method.

2. Results

A. TBX1 Gene Mutations

Whole genome sequencing was performed on III-C and a Gly387Ala_fs* heterozygous variant was identified in the TBX1 gene. This variant was also found in II-C, III-A, and III-B but not in II-D and III-D by Sanger sequencing. The mutation c.1158_1159delinsT was mapped to the TBX1 gene and was predicted to be of high impact variation, resulting in a frameshift by in-silico protein prediction algorithms and predicted to be present on protein TBX1-isoform C with a length of 495 aa. A mutation change from glycine to alanine was found at position 387 and with a stop codon at position 73, changing the protein length to 459 aa. No other mutations causing hypoparathyroidism were identified.

B. Predicted Effect

The TBX1-isoform C protein is 495 amino acids long, and the DNA-binding T-box domain is formed by residues 109–206 (18) (Fig. 2). The frameshift mutation results in a protein that deviates from TBX1-isoform C after residue 386, substituting the normal C-terminal 109-residue sequence with an unrelated sequence of 72 amino acids (Fig. 2A). The affected protein region is predicted to be unstructured, and hence, the mutation would not affect an existing 3D protein fold. The function of the replaced residues in TBX1 is unknown. However, the deleted region contains several sequence motifs that are predicted to serve as sites for protein interactions or posttranslational modifications (PTM). Importantly, the deleted region contains a nuclear localization sequence (NLS, residues 430–441) and a transactivation domain (TAD; localized within residues 409–495 (13) (Fig. 2). Combined deletion of these two functional regions has already been observed in DiGeorge syndrome patients and is likely also causing the phenotype observed here.
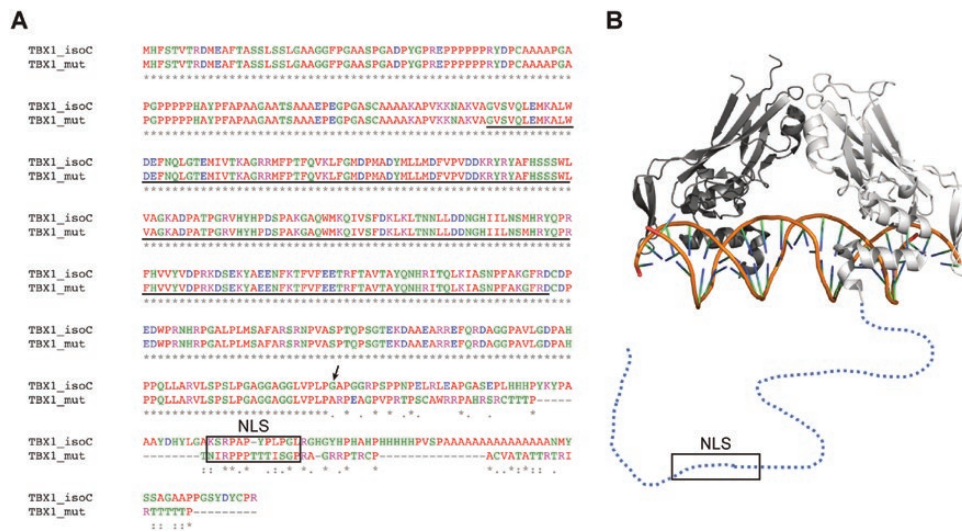
Figure 2. Effect of the p.(Gly387Alafs*73) mutation in the protein. (**A**) Color-coded sequence alignment of the TBX1-isoform C and its mutant sequence. The DNA-binding T-box domain is underlined. The position where wild-type and mutant deviate is indicated by an arrow. The NLS is indicated with a box. (**B**) Structural context of the mutation. The 3D structure of the TBX1 T- box dimer (dark and light gray) bound to DNA is shown (taken from PDB 4a04). For one molecule of the dimer, the flexible regions are illustrated by dashed (N-terminal) and dotted (C-terminal) lines. The arrow and boxed region show the approximal location of the mutation and NLS, respectively.

C. Gene Expression Studies

Our data revealed an unchanged gene expression by RT-PCR between the affected and nonaffected individuals; the predicted effect is a protein dysfunction that lacks NLS and TAD (Fig. 3).

3. Discussion

Craniofacial features and hypoparathyroidism were the presenting features in all affected family members, but deafness was a variable within the family that suggested an autosomal dominant inheritance. The lack of renal involvement in all four cases made HDR syndrome (hypoparathyroidism, sensorineural deafness, and renal disease) less likely, and the lack of conotruncal cardiac involvement and recurrent infections made DiGeorge syndrome less likely at the time of evaluation. Other causes of hypoparathyroidism are not typically associated with hearing loss, such as Kenny-Caffey type1 and type 2, Kearns-Sayre syndrome, familial hypercalciuric hypocalcemia, and isolated PTH gene defects will cause autosomal dominant and recessive hypothyroidism. Therefore, we assumed that we are dealing with a novel syndrome or a known syndrome with a novel presentation.

Whole genome sequencing identifies a high-impact novel variation resulting in a frameshift in the exon 9 TBX1 gene (Gly387Ala_fs*) that was co-segregated within the family. This report is the third to describe a variant affecting isoform C in the TBX1 gene that resulted in a 22q11.2 deletion–like phenotype. This mutation causes a shift of the reading frame, rearranging the PTM sites (S394 and R401), and most likely disturbing the T-box protein conformation, stability, and/or function. Additionally, both the nuclear localization signal (NLS) region (430–441 aa) and the transactivation domain (409–495) are 2 regions proceeding the frameshift that are likely to be abolished (Fig. 4), resulting in the inability of the protein to localize to the nucleus. Given that our data revealed an unchanged gene expression by RT-PCR between the affected and nonaffected individuals (Fig. 3), the predicted effect is a protein dysfunction that lacks NLS and TAD.
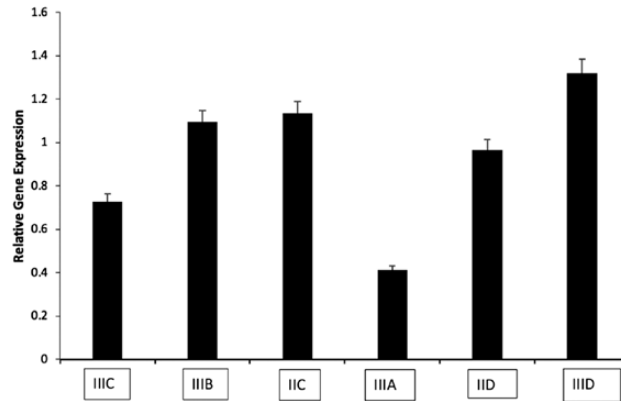
Figure 3. Relative expression of TBX1 mRNA.
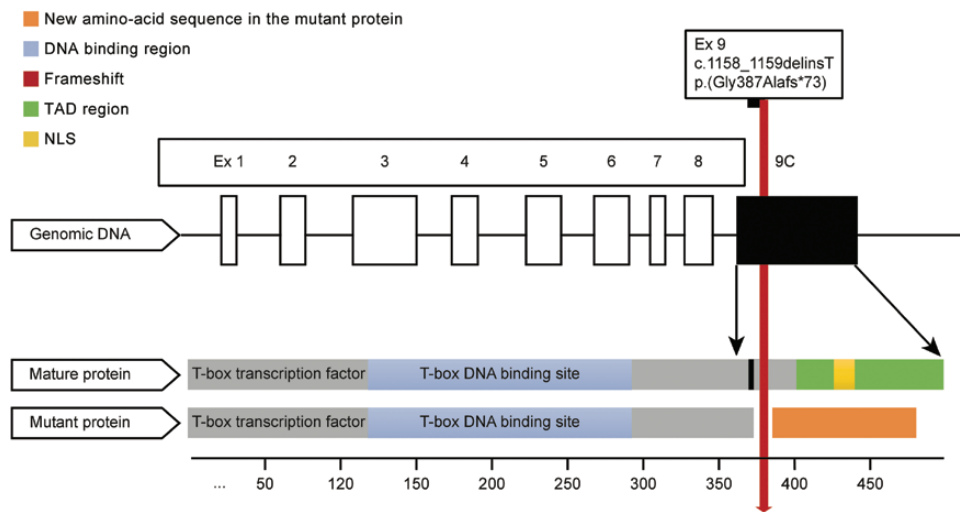
Figure 4. TBX1 gene from genomic to protein landscape displaying the mature protein length. Protein Domain Modeling is based on the mature protein with a length of 495 amino acids. Exhibited mutation change glycine to alanine on position 387 and with a stop-codon at position 73, changing the protein length to 459 amino acids. Both the nuclear localization signal (NLS) region (430–441 aa) and the transactivation domain (TAD) (409–495) are two regions proceeding the frameshift that are likely to be abolished.

Ogata et al (2014) described a Japanese family with a presentation similar to our family; the family had craniofacial changes and hypocalcemia with variable deafness, and the TBX1 variant was very close to the variant in our family (c.1253delA, p. Y418fsX459), producing a nonfunctional protein lacking NLS and most TAD (14). Additionally, Li et al (2018) reported a mutation that disrupted the NLS and TAD region and presented mostly with hypopara-thyroidism, and deafness presentation varied in these patients, similar to ours (15). Both of these families have no cardiovascular involvement, similar to ours. It seems that as long as the T-box is intact, there is no cardiac involvement. Yagi et al (2003) described a link be-tween the genotype and the phenotype by examining the type of mutated TBX1 transcripts (TBX1 A, TBX1B, and TBX1C), as reported in the family with the TBX1C mutation, which had a lower score of the 22q11.2 deletion phenotype (6). Our family is the third family that has a mutation affecting TBX1C transcripts and resulted in a 22q11.1 similar phenotype but without cardiac involvement.

Most likely, the TBX1-isoform C is the major functioning transcript isoform (8). In addi-tion to this characteristic feature, the TBX1 gene has other unique features, including: (1) the TBX1 gene acts as a dosage-sensitive transcription factor either as a gene enhancer or
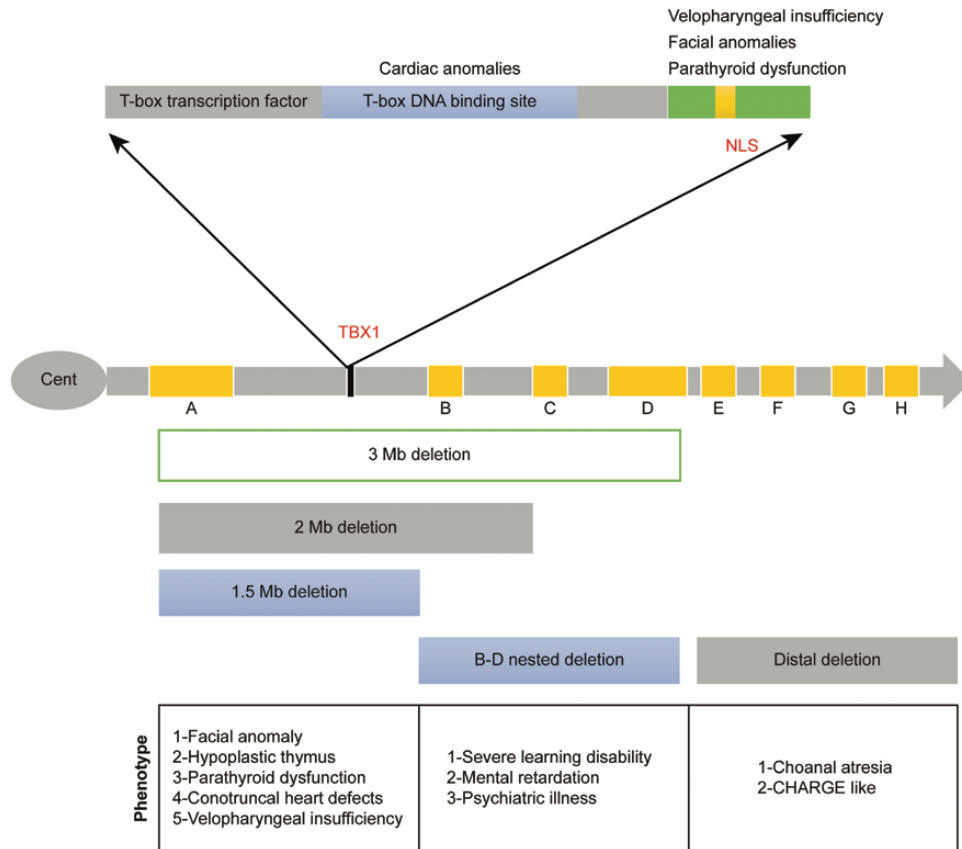
Figure 5. A correlation between the 22q11 deletion site / TBX1 gene mutation site and phenotypic expression. The bars below depict the site and the size of the 22q11 deletion and the associated clinical phenotype. The bar on the top depicts the location of the TBX1 gene pathogenic variant and the associated phenotype (21).

repressor, and is thus involved in the transcriptional regulation of developmental processes (12); (2) a specific genotype resulted in variable phenotype with significant intrafamilial and interfamilial variability, even among monozygotic twins (19), ranging from an asymptomatic heterozygous carrier, isolated nonsyndromic deafness, or isolated hypoparathyroidism to a DiGeorge-like phenotype (8–20), which indicates variable expressivity or reduced penetrance; (3) an autosomal dominant disorder with gain-of-function and loss-of-function variants disrupt gene function and result in a similar phenotype; and (4) the TBX1 gene is considered responsible for most clinical features in 22q11.2 deletion syndrome (12)

Few theoretical suggestions could explain the phenotypic variability in the TBX1 gene (21) (Fig. 5), including the genotype and phenotype correlation, for example, the loss of NLS and TAD domains is presented as a similar phenotype in our family and 2 other families, and the minor differences could be attributed to the level of disruption of these domains, variable expressivity, and reduced penetrance as well as environmental factors. Additionally, epigenetic changes might be considered in the future.

One of the limitations in our study is the absence of a functional study of the variants; hence, we are unable to prove the defect in nuclear localization.

In summary, DiGeorge syndrome caused by a pathogenic variant in the TBX1 gene is a rare autosomal dominant disease that is associated with a variable phenotype. We report a family of 4 members who presented with congenital hypoparathyroidism, facial dysmorphism, normal intelligence, deafness, and no cardiac involvement. Whole genome sequencing revealed a paternally-inherited novel heterozygous variant, c.1158_1159delinsT

p.(Gly387Alafs*73), in the exon 9 isoform C TBX1 gene, which we think is responsible for the phenotype within the family.

Acknowledgements

References

1. Kinouchi A, Mori K, Ando M, Takao A. Facial appearance of patients with conotruncal anomalies. *Pediatr Japan.* 1976;**17**:84.
2. Takao A, Masashiko A, Cho K, Kinouchi A, Murakami Y. Etiologic categorization of common congenital heart disease. In: Van Praagh R, Takao A, eds. *Etiology and Morphogenesis of Congenital Heart Disease.* New York: Futura; 1980:253–269.
3. Oskarsdóttir S, Vujic M, Fasth A. Incidence and prevalence of the 22q11 deletion syndrome: a population-based study in Western Sweden. *Arch Dis Child.* 2004;**89**(2):148–151.
4. Driscoll DA, Budarf ML, Emanuel BS. A genetic etiology for DiGeorge syndrome: consistent deletions and microdeletions of 22q11. *Am J Hum Genet.* 1992;**50**(5):924–933.
5. Jerome LA, Papaioannou VE. DiGeorge syndrome phenotype in mice mutant for the T-box gene, Tbx1. *Nat Genet.* 2001;**27**(3):286–291.
6. Yagi H, Furutani Y, Hamada H, et al. Role of TBX1 in human del22q11.2 syndrome. *Lancet.* 2003;**362**(9393):1366–1373.
7. Lindsay EA. Chromosomal microdeletions: dissecting del22q11 syndrome. *Nat Rev Genet.* 2001;**2**(11):858–868.
8. Gong W, Gottlieb S, Collins J, et al. Mutation analysis of TBX1 in non-deleted patients with features of DGS/VCFS or isolated cardiovascular defects. *J Med Genet.* 2001;**38**(12):E45.
9. Paylor R, Glaser B, Mupo A, et al. Tbx1 haploinsufficiency is linked to behavioral disorders in mice and humans: implications for 22q11 deletion syndrome. *Proc Natl Acad Sci U S A.* 2006;**103**(20):7729–7734.
10. Zweier C, Sticht H, Aydin-Yaylagül I, Campbell CE, Rauch A. Human TBX1 missense mutations cause gain of function resulting in the same phenotype as 22q11.2 deletions. *Am J Hum Genet.* 2007;**80**(3):510–517.
11. Griffin HR, Töpf A, Glen E, et al. Systematic survey of variants in TBX1 in non-syndromic tetralogy of Fallot identifies a novel 57 base pair deletion that reduces transcriptional activity but finds no evidence for association with common variants. *Heart.* 2010;**96**(20):1651–1655.
12. Baldini A. Dissecting contiguous gene defects: TBX1. *Curr Opin Genet Dev.* 2005;**15**(3):279–284.
13. Stoller JZ, Epstein JA. Identification of a novel nuclear localization signal in Tbx1 that is deleted in DiGeorge syndrome patients harboring the 1223delC mutation. *Hum Mol Genet.* 2005;**14**(7):885–892.
14. Ogata T, Niihori T, Tanaka N, et al. TBX1 mutation identified by exome sequencing in a Japanese family with 22q11.2 deletion syndrome-like craniofacial features and hypocalcemia. *Plos One.* 2014;**9**(3):e91598.
15. Li D, Gordon CT, Oufadem M, et al. Heterozygous Mutations in TBX1 as a Cause of Isolated Hypoparathyroidism. *J Clin Endocrinol Metab.* 2018;**103**(11):4023–4032.
16. Källberg M, Margaryan G, Wang S, Ma J, Xu J. RaptorX server: a resource for template-based protein structure modeling. *Methods Mol Biol.* 2014;**1137**:17–27.
17. Dinkel H, Van Roey K, Michael S, et al. ELM 2016–data update and new functionality of the eukaryotic linear motif resource. *Nucleic Acids Res.* 2016;**44**(D1):D294–D300.

18. El Omari K, De Mesmaeker J, Karia D, Ginn H, Bhattacharya S, Mancini EJ. Structure of the DNA-bound T-box domain of human TBX1, a transcription factor associated with the DiGeorge syndrome. *Proteins.* 2012;**80**(2):655–660.

19. Goodship J, Cross I, Scambler P, Burn J. Monozygotic twins with chromosome 22q11 deletion and discordant phenotype. *J Med Genet.* 1995;**32**(9):746–748.

20. McDonald-McGinn DM, Tonnesen MK, Laufer-Cahana A, et al. Phenotype of the 22q11.2 deletion in individuals identified through an affected relative: cast a wide FISHing net! *Genet Med.* 2001;**3**(1):23–29.

21. Rauch A, Zink S, Zweier C, et al. Systematic assessment of atypical deletions reveals genotype-phenotype correlation in 22q11.2. *J Med Genet.* 2005;**42**(11):871–876.

22. Hasegawa K, Tanaka H, Higuchi Y, et al. Novel heterozygous mutation in TBX1 in an infant with hypocalcemic seizures. *Clin Pediatr Endocrinol.* 2018;**27**(3):159–164.